Extreme Wave Loading on Offshore Wave Energy Devices using CFD: a Hierarchical Team Approach

J. Westphalen[1], D. M. Greaves[1], C. K. Williams[2], P. H. Taylor[3], D. M. Causon[4], C. G. Mingham[4], Z. Z. Hu[4], P. K. Stansby[5], B. D. Rogers[5] and P. Omidvar[5]

[1]PRIMaRE: Peninsula Research Institute for Marine Renewable Energy,
School of Engineering,
University of Plymouth,
Drake Circus, Plymouth, PL4 8AA, UK
E-mail: jan.westphalen@plymouth.ac.uk

[2]Department of Architecture and Civil Engineering,
University of Bath,
Bath, BA2 7AY, UK
E-mail: c.j.k.williams@bath.ac.uk

[3]Department of Engineering Science,
University of Oxford,
Parks Road, Oxford, OX1 3PJ, UK
E-mail: paul.taylor@eng.ox.ac.uk

[4]Department of Computing and Mathematics,
Manchester Metropolitan University,
Chester Street, Manchester, M1 5GD, UK
E-mail: Z.Hu@mmu.ac.uk

[5]School of Mechanical, Aerospace and Civil Engineering,
University of Manchester,
Manchester, M60 1QD, UK
E-mail: pourya.omidvar@postgrad.manchester.ac.uk

Abstract

Many different types of wave energy converters have been proposed in recent years. The two primary design considerations are the need to generate energy at competitive economic rates in average sea states and the need for the wave energy converters (WEC) to survive extreme wave conditions. Due to the complexity of most offshore wave energy devices and their motion response in different sea states, model scale tank tests are common practice for WEC design. Full scale tests are also necessary, but are expensive and only considered once the design has been optimised. Computational Fluid Dynamics (CFD) is now recognised as an important complement to traditional physical testing techniques in offshore engineering. Once properly calibrated and validated to the problem, CFD offers a high density of test data and results in a reasonable timescale to assist with design changes and improvements to the device. This paper deals with the results of test cases leading towards simulation of the full dynamics of Pelamis and the Manchester Bobber. The test cases presented involve the interaction between waves and fixed horizontal cylinders and results are compared with experimental data to validate the CFD codes. Also results for fluid-structure interaction of an oscillating cone on the water surface are presented. The surface elevation and diffraction effects are discussed, as well as the forces on the structures due to the waves and motion respectively. Four different CFD codes are applied to simulate the test cases: Smooth Particle Hydrodynamics, a Cartesian Cut Cell method based on an artificial compressibility method with shock capturing for the interface, and two pressure-based Navier-Stokes codes, one using a Finite Volume and the other a control volume based Finite Element approach.

Keywords: Cartesian-Cut-Cell, FEM, FVM, SPH, Wave-Structure Interaction

Nomenclature

A	=	Wave Amplitude or max. excursion
$\mathscr{A}$	=	Surface area
$\boldsymbol{B}$	=	Body force
CV	=	Control volume
d	=	Displacement
D	=	Diameter of cylinder
F	=	Force
$\boldsymbol{F}$	=	Flux vector function
g	=	Acceleration due to gravity
h	=	Waterlevel
k	=	Wavenumber
l	=	Length of cylinder
m	=	Integer between 1 and 12
n	=	Frequency component
$\boldsymbol{n}$	=	Normal vector
N	=	Number of frequency components
N_{KC}	=	Keulegan-Carpenter number
p	=	Pressure
$\boldsymbol{Q}$	=	Vector of conserved variables
r	=	Radius of cone at still water level
S	=	Source term
$\mathscr{S}$	=	Surface
t	=	Time
$\boldsymbol{u}$	=	Velocity vector
u,v,w	=	Components of $\mathbf{u}$
V	=	Domain of interest
$\mathscr{V}$	=	Volume of CV or particle
W	=	Weighting function
$\boldsymbol{x}$	=	Position vector
x,y,z	=	Coordinate directions
β	=	Coefficient of artificial compressibility
Γ	=	Diffusion coefficient
Δt	=	Timestep
$\Delta\omega_n$	=	Frequency step
ρ	=	Density
ϕ	=	General flow property
Φ	=	Flow property gradient
μ	=	Viscosity
η	=	Surface elevation
ω	=	Frequency
∇	=	Gradient

Subscripts

0	=	Initial
a	=	Particle
b	=	at boundary
h	=	Smoothing kernel
i,j	=	mid point
n	=	Frequency component
rms	=	Root mean square
t	=	Time
x,y,z	=	Coordinate directions
ϕ	=	General flow property

Superscripts

$'$	=	relative

1 Introduction

In recent years the necessity for sustainable energy has become a topic, which is addressed almost everywhere in everyday-life. For example, many car manufacturers are developing low emission or fuel cell powered vehicles and efforts are being made to incrase energy efficiency in buildings. The European Governments have the reduction of CO_2 emissions on their agenda. For example, the UK aim to cut the volume of carbon dioxide blown in the atmosphere by 20% by 2010 relative to 1990 levels. In offshore engineering wave and tidal energy is available in almost unlimited resources, which makes this area very interesting for a contribution to European renewable energy targets. The major drawback still is the high cost of developing such technologies, and especially operating offshore. High strains act on every structure at sea, making survivability a key design driver. Maintenance is difficult due to harsh weather conditions and highly qualified staff and specialist equipment is expensive.

CFD provides a design tool, both cost effective and accurate, that can help to reduce the overall design costs of such wave energy converters (WEC). The UK based and EPSRC funded project "Extreme Wave Loading on Offshore Wave Energy Devices using CFD" follows a hierarchical approach. In this project, four different CFD techniques are being applied to simulate two WECs: Pelamis and the Manchester Bobber.

The ultimate aim of the simulations is to investigate the very complex dynamics of these devices with multi-body-wave interaction and 6-degree-of-freedom motion using different CFD techniques. Towards this aim, a number of test problems of increasing complexity are being investigated. Wave-wave interaction has successfully been modelled [1]. This paper focusses on wave-structure interaction. The four computational techniques, i.e. Smooth Particle Hydrodynamics (SPH), a Cartesian Cut Cell method based on an artificial compressibility method with shock capturing for the interface (AMAZON), and two pressure-based Navier-Stokes codes, one using a Finite Volume (FV) and the other a control volume Finite Element approach (CV-FE), are applied to a fixed cylinder case and also to one simulation involving motion.

First, regular waves interacting with a fixed horizontal cylinder are modelled. Here the forces generated by the waves are analysed. Next, the simulation of a cone-shaped body near the water surface is discussed, in which the interaction between the cone and water is reduced to act in a single direction. As the cone is oscillating at the water surface following the motion of a Gaussian wave packet, the motion is independent of the forces generated at the surface by the surrounding water. Here the vertical forces on the cone surface are of interest and the relative water surface elevation near the cone is discussed.

2 Mathematical Models

2.1 Finite Volume

The Finite Volume solver uses the Navier-Stokes equations discretised on a 3-dimensional mesh to calculate the velocities and pressures in the flow field in a segregated iterative way. The flow is described by the equation of mass conservation as

$$\frac{\partial u}{\partial x}+\frac{\partial v}{\partial y}+\frac{\partial w}{\partial z}=0, \tag{1}$$

and the three momentum equations as

$$\frac{\partial u\rho}{\partial t}+\operatorname{div}(\rho u\boldsymbol{u})=-\frac{\partial p}{\partial x}+\operatorname{div}(\mu \operatorname{grad} u)+S_x, \tag{2}$$

$$\frac{\partial v\rho}{\partial t}+\operatorname{div}(\rho v\boldsymbol{u})=-\frac{\partial p}{\partial y}+\operatorname{div}(\mu \operatorname{grad} v)+S_y \tag{3}$$

and

$$\frac{\partial w\rho}{\partial t}+\operatorname{div}(\rho w\boldsymbol{u})=-\frac{\partial p}{\partial z}+\operatorname{div}(\mu \operatorname{grad} w)+S_z. \tag{4}$$

u, v and w are the components of the velocity vector $\boldsymbol{u}$ pointing in x, y and z direction, respectively. ρ is the fluid density, p the pressure, μ the fluid viscosity and t stands for the time. S_i, with i being x, y or z, is the source term acting in i-direction, in which e.g. gravity forces are included. In integral form equations (1), (2), (3) and (4) can be rewritten as the general transport equation

$$\int_{\Delta t}\frac{\partial}{\partial t}\left(\int_{CV}\rho\phi d\mathscr{V}\right)dt+\int_{\Delta t}\int_{\mathscr{A}}\boldsymbol{n}.(\rho\phi\boldsymbol{u})\,d\mathscr{A}\,dt=$$

$$\int_{\Delta t}\int_{\mathscr{A}}\boldsymbol{n}.(\Gamma\operatorname{grad}\phi)\,d\mathscr{A}\,dt+\int_{\Delta t}\int_{CV}S_\phi d\mathscr{V}dt, \tag{5}$$

which is the starting point for the solution by the Finite Volume method. ρ is the fluid density, ϕ is the transported flow property such as velocity or pressure, Γ is the diffusion coefficient, $\mathscr{A}$ is the surface area of the control volumes (CV) face, $\mathscr{V}$ is the volume of the CV and S_ϕ is the source term. $\boldsymbol{n}$ is the vector normal to a CV face and $\boldsymbol{u}$ is the velocity vector.

The domain, here a numerical wave tank (NWT) including the structure, i.e. a horizontal cylinder or a cone shaped body at the water surface, is subdivided into discrete volumes. The surface and volume integrals (5) performed on the control volumes are used to calculate the variable values at the centre node of the CV. This approach makes the Finite Volume method conservative by construction. Calculations are performed for both fluids, i.e. water and air, using the well known Volume of Fluid (VoF) method. For the CVs containing the fluid interface the CISCAM scheme, described by [2–4], is applied.

2.2 Control-Volume Finite Element

The control-volume Finite Element approach combines the Finite Volume method considering the control volumes and the Finite Element method by using shape functions and a different discretisation scheme. The shape functions are used to calculate the change of a variable across the CV [5–7]. As described for the Finite Volume method in 2.1 the CV-FE also solves the Navier-Stokes equations for incompressible fluids. The general transport equation as stated in (5) is discretised on a 3-dimensional grid containing hexahedral cells. The CVs are arranged around the mesh nodes and thereby this technique ensures the conservation of flow quantities such as mass and momentum. In all simulations the fluid fractions of air and water are solved using the Volume of Fluid formulation. The fluid interface is treated by the method described by [5, 8–10], which is dependent on the filling level of the surrounding cells rather than the Courant number as in [2]. This solver is used for the horizontal and vertical cylinder cases and also the oscillating cone. The latter involves motion, which is modelled by moving the nodes and edges of the mesh at the beginning of each timestep before the fluid dynamics are solved.

2.3 Smooth Particle Hydrodynamics

Smoothed Particle Hydrodynamics (SPH) is a flexible Lagrangian technique for computational fluid dynamics simulations. In this method the fluid system is represented by a set of particles which have individual material properties and move according to governing conservation equations [11]. There is no mesh construction in SPH, therefore in certain problems, for instance simulation of waves, the SPH method may be easier to develop and use than Eulerian methods. The value of a flow quantity Φ at a position vector $\boldsymbol{x}$ is approximated as

$$\Phi(\boldsymbol{x})=\sum_j\Phi_jW_h(\boldsymbol{x}-\boldsymbol{x}_j)\mathscr{V}_j \tag{6}$$

where $\mathscr{V}_j$ is the volume of the j-th particle located at $\boldsymbol{x}_j$ with scalar quantity Φ_j, and W_h is the weighting function referred to as the smoothing kernel, h. The differentiable form of the interpolant of the function ϕ according to 6 leads the kernel function to be also differentiable. Therefore, one can write the gradient of the scalar field Φ relative to the particle as

$$(\nabla\Phi)_i=\sum_j(\Phi_j-\Phi_i)\nabla_iW_h(\boldsymbol{x}_i-\boldsymbol{x}_j)\mathscr{V}_j. \tag{7}$$

To simulate water, the fluid is allowed to be weakly compressible using an artificial equation of state [11] so that the time step is not prohibitively small. The simulations are run using the open source code SPHysics [12]. The symplectic algorithm [13], often known as kick-drift-kick, is used as the time stepping method. Following the work of Vila [14], the governing equations for compressible Navier-Stokes flow written in SPH form include position, conservation of mass and momentum:

$$\frac{\partial\boldsymbol{x}_i}{\partial t}=\boldsymbol{u}(\boldsymbol{x}_i,t) \tag{8}$$

$$\frac{\partial}{\partial t}\left(\mathscr{V}_i\rho_i\right)+\mathscr{V}_i\sum_{j\in p}\mathscr{V}_j 2\rho_a\left(\boldsymbol{u}_{a,ij}-\boldsymbol{u}^0\left(\boldsymbol{x}_{ij},t\right)\right)\cdot\nabla_i W_{ij}=0 \tag{9}$$

$$\frac{\partial}{\partial t}\left(\mathscr{V}_i\rho_i v_i\right)+ \mathscr{V}_i\sum_{j\in p}\mathscr{V}_j 2\left[\rho_a+\rho_a\boldsymbol{u}^0_{a,ij}\otimes\left(\boldsymbol{u}^0_{a,ij}-\boldsymbol{u}^0\left(x_{ij},t\right)\right)\right]\nabla_i W_{ij}=\mathscr{V}_i S_i \tag{10}$$

where all the symbols have their usual meaning with $\mathscr{V}_i$ being the volume of the i-th particle, and S_i is the body force. The interaction between each particle pair is solved as a Riemann problem, so that the solution at the mid-point, x_{ij}, is $\boldsymbol{u}^0_{a,ij}$, p_a, ρ_a for velocity, pressure and density respectively. The scheme is rendered second order accurate using TVD reconstruction and there is no explicit viscosity formulation in the model.

The repulsive boundary condition, developed by Monaghan [15] and modified by [16], is used which prevents a water particle crossing a solid boundary. This technique is used to simulate the horizontal cylinder cases. By the principle of equal and opposite reaction, the forces on the cylinder can be estimated by summing the forces exerted on the body particles by water particles. The dimensionless force F' is determined as the ratio of wave force to the weight of water displaced by a totally submerged cylinder in still water to compare with experimental data.

2.4 Cartesian-Cut-Cell

The AMAZON-3D numerical wave tank (NWT) for a study of wave loading on a wave energy converter (WEC) device has been developed in MMU, which is based on the free surface capturing method for two fluid flows with moving bodies developed by [17], which demonstrated a rigid 2D wedge-shaped body entering calm water and its subsequent total immersion. The NWT, based on a two fluid free surface capturing and Cartesian cut cell method, is being developed for the simulation of wave loadings on the Manchester Bobber device under extreme wave conditions.

The AMAZON-3D code uses a Cartesian cut cell method to provide a boundary-fitted grid for both static and moving boundaries in 3D. The main advantages of the Cartesian cut cell approach has been outlined previously [18, 19], including particularly its flexibility for dealing with complex geometries and moving bodies. There is no requirement to re-mesh globally or even locally for a moving boundary problem which only requires changes locally at cells in the background Cartesian mesh that are cut by the moving boundary contour. The AMAZON-3D code has been extended to handle a 3D floating bobber moving in the vertical direction in extreme waves. For this paper, however, the code is applied to a fixed horizontal cylinder and the simulation of a cone shaped body, which oscillates at the water surface.

The AMAZON-3D code is based on the integral form of the Euler equations for 3D incompressible flow with variable density in integral form and can be written as

$$\frac{\partial}{\partial t}\iiint_V \boldsymbol{Q}dV+\oint_{\mathscr{S}}\boldsymbol{F.n}d\mathscr{S}=\iiint \boldsymbol{B}dV \tag{11}$$

where $\boldsymbol{Q}$ is the vector of conserved variables which encloses the time dependent domain of interest V , $\boldsymbol{F}$ is the flux vector function and $\boldsymbol{n}$ is the outward unit vector normal to the boundary $\mathscr{S}$. $\boldsymbol{B}$ is a source term for body forces. $\boldsymbol{Q}$, $\boldsymbol{F}$ and $\boldsymbol{B}$ are given by

$$\boldsymbol{Q}=\left[\rho,\rho u,\rho v,\rho w,p/\beta\right]^T, \tag{12}$$

$$\boldsymbol{F}=f^I n_x+g^I n_y+h^I n_z \tag{13}$$

and

$$\boldsymbol{B}=\left[0,0,0,-\rho g,0\right]^T, \tag{14}$$

with

$$f^I=\begin{bmatrix}\rho\left(u-u_b\right)\\ \rho u\left(u-u_b\right)+p\\ \rho v\left(u-u_b\right)\\ \rho w\left(u-u_b\right)\\ u\end{bmatrix}, \tag{15}$$

$$g^I=\begin{bmatrix}\rho\left(v-v_b\right)\\ \rho u\left(v-v_b\right)\\ \rho v\left(v-v_b\right)+p\\ \rho w\left(v-v_b\right)\\ v\end{bmatrix}, \tag{16}$$

$$h^I=\begin{bmatrix}\rho\left(w-w_b\right)\\ \rho u\left(w-w_b\right)\\ \rho v\left(w-w_b\right)\\ \rho w\left(w-w_b\right)+p\\ w\end{bmatrix}, \tag{17}$$

where u, v and w are the flow velocity components and u_b , v_b and w_b are the velocity components of the boundary $\mathscr{S}$, which are zero when the boundary is stationary. ρ is the density, p is the pressure, β is the coefficient of artificial compressibility and g is the gravitational acceleration.

The free surface is treated as a contact surface in the density field that is captured automatically during a time-marched calculation without special provision in a manner analogous to shock capturing in compressible flow. A time-accurate artificial compressibility method and high resolution Godunov-type scheme replaces the pressure correction solver used in many current VoF methods. AMAZON-SC can handle break-up and recombination of the free surface as well as air entrainment into the water and, in principle, associated local compressibility effects. The total force is obtained by integration of the pressure field along the body $F=-\int_{S_b}p\boldsymbol{n}dS$, where S_b is the body surface and is defined by the cut cell surface.

3 Horizontal Cylinder

The first set of tests concern a fixed horizontal cylinder described by [20]. The authors carried out physical tank tests in order to improve Morison's formula for the calculation of the forces on a horizontal cylinder. For different levels of submergence and wave amplitudes they recorded the vertical forces acting on the cylinder due to the waves. Here, all four numerical techniques were applied to several tests and compared with the experimental results [20].

The forces calculated using each of FV, CV-FE, SPH and AMAZON are compared for several different wave amplitudes and cylinder axis depths as it can be seen in Tables 1 and 2. The relative amplitude A' and axis depth or displacement d' are defined as the ratios between either the amplitude A or axis depth d and the cylinder diameter D, respectively. To compare the numerical results with those obtained by Dixon *et al.* [20] the vertical forces F_z on the cylinder resulting from drag and pressure on the surface are exported. The forces F_z' shown in all figures are non-dimensionalised using the following expression

$$F' = \frac{F_z}{g\rho\left(1/4\pi D^2 l\right)} \tag{18}$$

with F_z being the measured vertical force on the cylinder, g the acceleration due to gravity, ρ the density of water, D the cylinder diameter and l the length of the cylinder. As in the physical experiment 1st order regular waves are generated in the NWT to hit the structure. For the FV and CV-FE approach the wave velocity components u and w and the surface elevation η as described by

$$u = \frac{gAk\cosh\left(k\left(z+h\right)\right)\cos\left(kx-\omega t\right)}{\omega\cosh\left(kh\right)}, \tag{19}$$

$$w = -\frac{gAk\sinh\left(k\left(z+h\right)\right)\sin\left(kx-\omega t\right)}{\omega\cosh\left(kh\right)} \tag{20}$$

and

$$\eta = A\cos\left(kx-\omega t\right). \tag{21}$$

are applied for the water fraction at the upstream end of the 3-dimensional NWT using a velocity inlet boundary condition. The velocities for the air fraction are set to 0.0m/s. The top boundary is a pressure outlet, the sides are modelled as symmetry planes and the bottom, the cylinder and downstream end of the domain are defined as walls. The total number of cells for the FV meshes are 113856, 113606 and 114599. The CV-FE meshes contain 79495, 69537 and 695375 cells. The number of cells on the cylinder itself however is 250 for the FV solver and 236 for CV-FE. The timestep to achieve a converged solution is set to 0.001 s and 0.05 s for FV and CV-FE respectively. Figures 1 and 2 show a section of the meshes used for the Navier-Stokes solvers for the relative axis depth d' of 0.0, where the centre of the cylinder sits at still water level.

In AMAZON, the left-hand boundary condition is a velocity inlet, where (19), (20) and (21) are applied for the water fraction to generate the wave in the domain. The air part of the left-hand boundary and the top and right boundary are specified as non-reflecting boundary conditions allowing air to leave or enter the domain. The cylinder surface is defined as a reflective wall boundary. The remaining sides are slip boundaries. The NWT contains 438850 cells with a minimum edge length of 0.015m. A timestep of 0.00025s is applied.

For the SPH method the calculations are carried out in a 2-dimensional NWT using 13000 particles in the domain. The boundaries are treated as walls, i.e. the wavemaker, the bottom, the downstream end and the cylinder. The waves are generated by moving the upstream wall similar to a piston wavemaker.

In Figures 3 and 5 the time histories of the non-dimensionalised vertical forces over one wave period are shown for AMAZON, and the two Navier-Stokes solvers. For d' = 0.0 and A' = 0.5 the three codes give very good agreement with the experimental data. For d' = -0.3 and A' = 0.2 the results look even better. Fig. 4 shows the surface elevation around the cylinder ($d' = 0.0$) for different times for the FV solver. Especially for t/T = 0.6 and 0.73 air entrainment can be observed. For the fully submerged case shown in Fig. 6 the relative forces calculated by CFD differ somewhat from the physical experiment. Although the computational results agree in quantity, the phases do not match between FV, CV-FE and the physical experiment.

Table 1: Properties of Horizontal Cylinder Simulations for FV, CV-FE and AMAZON (simulation 1 and 2 only)

	Simulation		
	1	2	3
d' [m]	0.0	-0.3	-0.6
A' [m]	0.5	0.2	0.3
kA	0.2	0.01	0.12
kh	1.61	1.61	1.61
N_{KC}	3.1	1.3	1.9

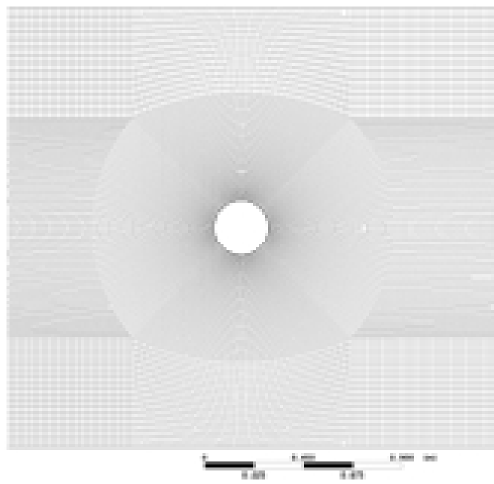

Figure 1: CV-FE Mesh Section around Cylinder

Fig. 7 shows the particle distributions at different times for the SPH method. The wave propagation near

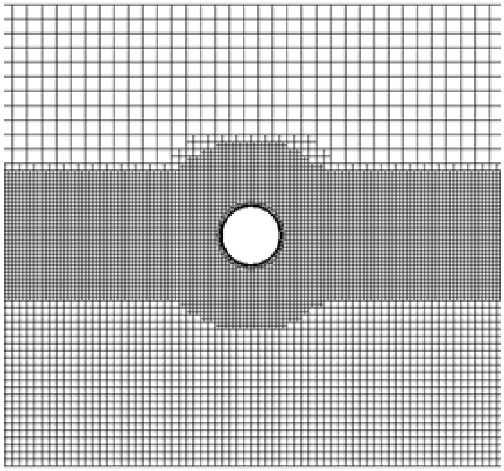

Figure 2: FV Mesh Section around Cylinder

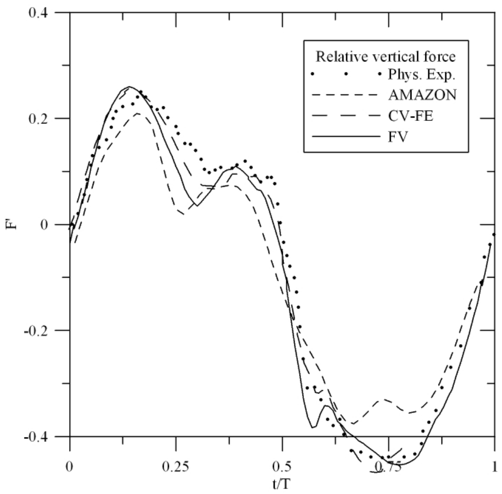

Figure 3: Relative vertical forces on horizontal cylinder (d' = 0.0, A' = 0.5)

the cylinder has clearly been altered by the presence of the cylinder. Since the simulations are mono-phase (i.e. only water particles) the compressibility of air around the cylinder is not taken into account. To compare the forces obtained by the SPH method with the experimental data, the root mean square vertical force is calculated as

$$F_{rms} = \sqrt{\frac{1}{n}\sum_{n=1}^{n} F_i^2} \tag{22}$$

where F_{rms} is the root mean square force, F_i is the total force component at each time step (evaluated by summing the force contribution from nearby fluid particles) and n is the number of time step.

Table 2 shows the comparisons of dimensionless rms force between the SPH results and the experimental data presented by [20] for different relative axis depths and relative amplitudes. As shown in the table, one can see that the experimental and SPH results are in reasonable agreement especially for the half submerged cylinder where the interaction between fluid particles and body particles are less than the fully submerged case. For the submerged cylinder, the results also show promising agreement but with a discrepancy that might be due to problems with the experimental data.

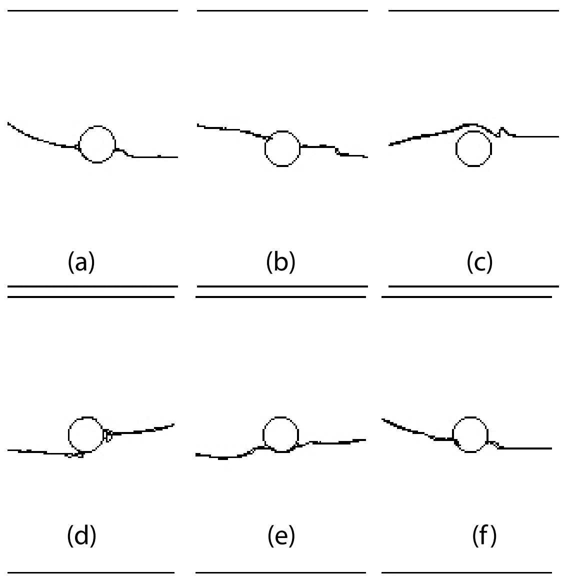

Figure 4: Surface elevation around cylinder, d' = 0.0, A' = 0.5; (a) t/T= 0.0, (b) t/T= 0.12, (c) t/T= 0.36, (d) t/T= 0.6, (e) t/T= 0.73, (f) t/T= 1.0.

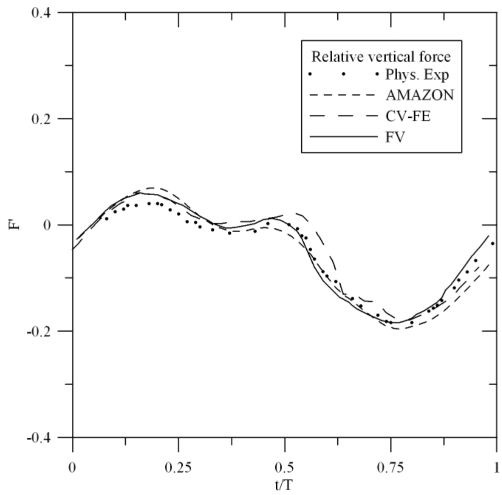

Figure 5: Relative vertical forces on horizontal cylinder (d' = -0.3, A' = 0.2)

4 Oscillating Cone

For the simulation of floating bodies, the authors' main interest lies in Pelamis and the Manchester Bobber, so it is important to be able to calculate the forces on a moving body and the surface elevations around it correctly. For the purpose of the validation of the codes a simplified test setup accommodating a cone shaped body near the water surface is chosen. The motion of the cone is driven and not influenced by the forces generated on its surface by the surrounding fluids. The physical tank tests are described in [21]. In the experiments, the vertical forces on the cone surface due to its motion and the relative water surface elevation at a distance of 0.03m from the cone surface were recorded. Here comparisons between AMAZON, the CV-FE solver and the physical

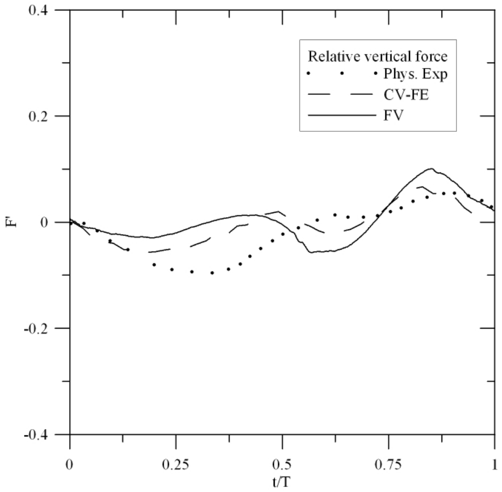

Figure 6: Relative vertical forces on horizontal cylinder (d' = -0.6, A' = 0.3)

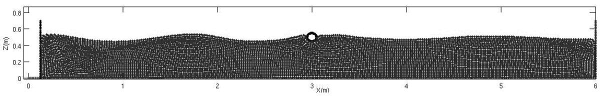

(a) t = 5s

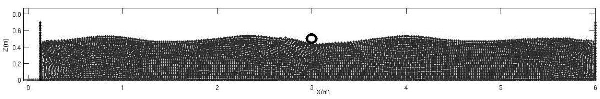

(b) t = 7.5s

Figure 7: Particle configuration for half submerged cylinder with the relative amplitude of 0.5 at

experiments are shown.

The motion of the cone is defined by the displacement $d(t)$ from the initial position at t = 0s following the form of a Gaussian wave packet, which is described by

$$d\left(t\right) = A\sum_{n=1}^{N} Z\left(\omega_n\right)\cos\left[\omega_n\left(t-t_0\right) - \frac{h\pi}{2}\right]\Delta\omega_n, \quad (23)$$

where

$$Z\left(\omega_n\right) = \frac{1}{\frac{\omega_n}{2\pi}\sqrt{2\pi}}\exp\left[-\frac{\left(\omega_n-\omega_0\right)^2}{2\left(\frac{\omega_0}{2\pi}\right)^2}\right] \quad (24)$$

with h = 0 or 1. A denotes the largest excursion from the

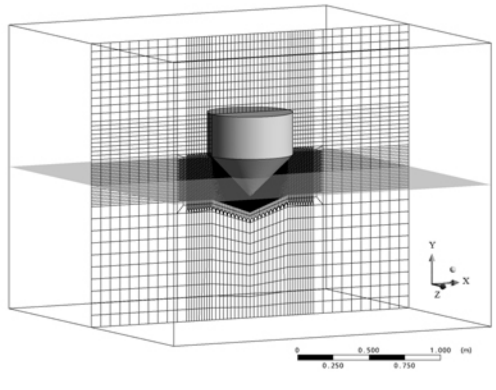

Figure 8: Computational domain used for CV-FE with mesh and position of initial water surface

Table 2: Comparison of SPH rms force, normalised by submerged buoyancy force, with experiment for different relative wave amplitude and axis depth

A'	d'	SPH F_{rms}	Exp. F_{rms}
0.10	0	0.075	0.062
0.50	0	0.259	0.264
0.20	-0.1	0.115	0.112
0.20	-0.2	0.120	0.101
0.20	-0.3	0.109	0.087
0.30	-0.4	0.149	0.118
0.30	-0.5	0.179	0.089

still water level. N is the number of frequency components and ω_n is the appropriate circular frequency. The central circular frequency ω_0 [rad/s] is defined by

$$\omega_0 = \frac{m\pi}{3} \quad (25)$$

with m being an integer between 1 and 12.

For the CV-FE approach the simulations are performed in a three-dimensional domain with a length and width of 2.5m and a height of 2.0m. The cone is placed in the centre, as it can be seen in Fig. 8. It has a top diameter of 0.6m and a steepness of the deadarise angle of 45. The slope itself is 0.3m high. The initial draught of the cone is 0.15m at a waterdepth of 1.0m. The cone is modelled as a cavity in the mesh. The outer boundaries, the bottom and the cone are modelled as free slip walls. The top boundary is defined as a pressure outlet with constant atmospheric pressure. The mesh consists of 820,000 hexahedral cells, where the regions around the water surface and the cone surface are highly refined to achieve cell edges of approximately 0.01m. The outer regions are relatively coarse to save computational resources and encourage numerical damping, thus avoiding reflections from the walls. The simulations were carried out using high performance computing on 16 CPUs. The timestep is 0.0005s.

In AMAZON a 2m x 1.6m axisymmetric domain is used. The still water level is set to 1.02m and the initial draught of the cone is 0.148m. The calculations are performed on a hexahedral grid using an axisymmetric (2D) version of the code with cell sizes of 0.02 x 0.02m. The timestep is 0.00005s. The exported vertical forces F_z from the CFD codes are non-dimensionalised using the expression

$$F'(t) = \frac{F_z(t)}{\rho g\pi r^2 A} \quad (26)$$

with ρ being the density of fresh water, g the acceleration due to gravity, r the cone radius at still water level and A the maximum excursion. Also the time is divided by the corresponding period of the central frequency ω_0. The measured relative motion of the water surface is divided though the maximum excursion A = 0.05m.

Fig. 9 compares the force data obtained by AMAZON and the CV-FE solver with those of the physical experiment. Generally the agreement is satisfactory. Both codes generate little differences especially in the force minima and maxima. AMAZON slightly overestimates the forces and the Navier-Stokes solver underestimates them. Looking at the relative motion of the free surface at the cone for this experiment shown in Fig. 10, the differences become larger. Here, both codes generate results, which are smaller in the crests and larger in the troughs. this difference is currently under investigation and may be due to the difficulty in generating an orthogonal mesh for a body with sloping sides at the free surface.

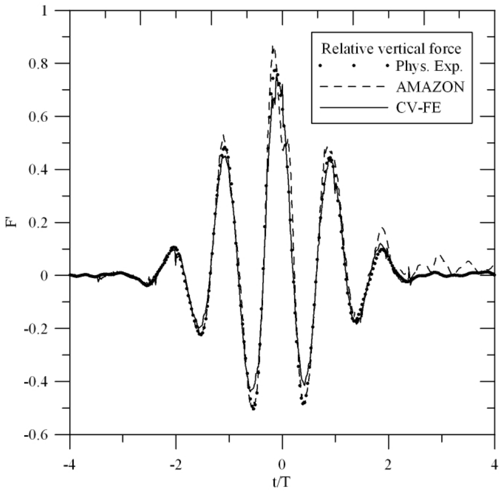

Figure 9: Relative vertical force on cone

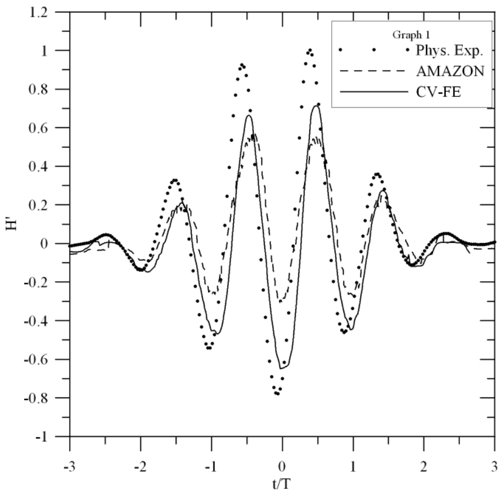

Figure 10: Relative surface motion at cone

5 Conclusions

Results are presented for four different computational methods, i.e. SPH, a Cartesian Cut Cell method and two pressure-based Navier- Stokes codes, one using a Finite Volume and the other a control volume based Finite Element approach. These were applied to cases involving fluid structure interaction with a fixed horizontal cylinder in different wave conditions and levels of submergence. Also results for an experiment including motion of the structure are shown. All the numerical simulations show good overall agreement with the experimental results they are compared with.

The investigation of the horizontal cylinder shows that all solvers calculate the forces on the structure well for axis displacements d' = 0.0 and d' = -0.3. Here the pressures and shear stresses are in good agreement with measurements in the physical tank test. For the fully submerged cases with d' smaller than -0.5 the numerical results in all solvers generate differences. The FV and CV-FE methods can predict the forces quantitatively, but the quality of the time histories is different. For the SPH method the root mean squares were analysed, which give the same trend with good agreement for the cases with the cylinder axis closer to the water surface.

The CV-FE and AMAZON solvers performed well on the oscillating cone case. The main design interest for WEC probably lies in the calculation of the forces acting on the structure. These are in very good agreement. The prediction of the free surface at the body boundary can still be improved however. For the CV-FE method this is believed to occur due to mesh effects coming from non-vertical and -horizontal cell edges aggravated by the very small body displacement in the test case. This will be investigated further in both codes and also using the FV solver and SPH.

The outcome so far shows, that all the applied computational techniques are very powerful tools. The Cartesian-Cut-Cell method (AMAZON), SPH and the two Navier-Stokes solvers, i.e. the FV and CV-FE approach, perform well in all experiments they were applied to.

Acknowledgements

The authors would like to acknowledge the support of the Engineering and Physical Sciences Research Council.

References

[1] J. Westphalen, D. Greaves, C. Williams, J. Zang, and P. H. Taylor. Numerical simulation of extreme free surface waves. In *Proceedings of the 18th International Offshore and Polar Engineering Conference*, Vancouver, Canada, 2008.

[2] O. Ubbink. *Numerical prediction of two fluid systems with sharp interfaces*. PhD thesis, Imperial College of Science, Technology & Medicine, 1997.

[3] J.H. Ferziger and M. Peric. *Computational Methods for Fluid Dynamics*. Springer, Heidelberg, 3rd edition, 2001.

[4] CD-Adapco. *STAR CCM+ Version 3.02.003*. User Guide. London, UK, 2008.

[5] Ansys Inc. *ANSYS CFX-Solver Theory Guide*. ANSYS CFX - Release 11.0. Canonsburg, USA, 2006.

[6] B.R. Baliga and S.V. Patankar. A control volume finite-element method for two-dimensional fluid flow and heat transfer. *Numerical Heat Transfer, Part A*, 6:245–261, 1983.

[7] B.R. Baliga and S.V. Patankar. A new finite-element formulation for convection-diffusion problems. *Numerical Heat Transfer, Part A*, 3:393–409, 1980.

[8] J.T. Barth and D.C. Jesperson. The design and application of upwind schemes on unstructured meshes, 1989.

[9] P.J. Zwart. Numerical modelling of free surface and cavitating flows. Technical report, Ansys Canada Ltd., 2005.

[10] P.J. Zwart, M. Scheuerer, and M. Bogner. Free surface modelling of en impinging jet, September 15-16 2003 2003.

[11] J. J. Monaghan. Smoothed particle hydrodynamics. *Reports on Progress in Physics*, 68(8):1703–1759, August 2005.

[12] SPHysics. http://wiki.manchester.ac.uk/sphysics, 2009.

[13] B. J. Leimkuhler, S. Reich, and R. D. Skeel. Integration methods for molecular dynamics. In *Mathematical Approaches to Biomolecular Structure and Dynamics, IMA Volumes in Mathematics and its Applications*, pages 161–185. Springer, 1994.

[14] J. P. Vila. On Particle Weighted Methods and Smoothed Particle Hydrodynamics. *Mathematical Models and Methods in Applied Sciences*, 28(3):395–418, 1999.

[15] J. J. Monaghan and A. Kos. Solitary waves on a creatan beach. *J. of Waterway, Port, Coastal and Ocean Engineering*, 125(8):145–154, 1999.

[16] B.D. Rogers and R.A. Dalrymple. Sph modeling of tsunami waves. In *Advances in Coastal and Ocean Engineering, Vol. 10 Advanced Numerical Models for tsunami waves and runup*. World Scientific, 2008.

[17] L Qian, D.M Causon, C.G Mingham, and D.M Ingram. A free-surface capturing method for two fluid flows with moving bodies. *Proceedings of the Royal Society A: Mathematical, Physical and Engineering Science*, 462(2065):21–42, 2006.

[18] D. M. Causon, D. M. Ingram, C. G. Mingham, G. Yang, and R. V. Pearson. Calculation of shallow water flows using a cartesian cut cell approach. *Advances in Water Resources*, 23(5):545–562, February 2000.

[19] D. M. Causon, D. M. Ingram, and C. G. Mingham. A cartesian cut cell method for shallow water flows with moving boundaries. *Advances in Water Resources*, 24(8):899–911, August 2001.

[20] A.G. Dixon, C.A. Greated, and S.H. Salter. Wave forces on partially submerged cylinders. *Journal of the Waterway, Port, Coastal and Ocean Devision*, 105(4):421–438, 1979.

[21] K. Drake, R. Eatock Taylor, P. Taylor, and W Bai. On the hydrodynamics of bobbing cones. *submitted for publication*, 2008.